On the Efficiency of Capacitively-Loaded Frequency-Reconfigurable Antennas

Barrio, Samantha Caporal Del; Pedersen, Gert Frølund

Published in:
International Journal of Distributed Sensor Networks

DOI (link to publication from Publisher):
10.1155/2013/232909

Publication date:
2013

Document Version
Early version, also known as pre-print

Hindawi Publishing Corporation
International Journal of Distributed Sensor Networks
Volume 2013, Article ID 232909, 8 pages
http://dx.doi.org/10.1155/2013/232909

Research Article

On the Efficiency of Capacitively Loaded Frequency Reconfigurable Antennas

Samantha Caporal Del Barrio and Gert F. Pedersen

Section of Antennas, Propagation and Radio Networking (APNet), Department of Electronic Systems, Faculty of Engineering and Science, Aalborg University, 9220 Aalborg, Denmark

Correspondence should be addressed to Samantha Caporal Del Barrio; scdb@es.aau.dk

Received 27 February 2013; Accepted 10 June 2013

Academic Editor: Korkut Yegin

The design of a reconfigurable antenna that can be fine tuned to address future communication systems is proposed. The design consists of a capacitively loaded patch antenna for nowadays smartphone platforms. The antenna is narrowband and can be fine tuned over the range (700 MHz–960 MHz). Measurements at 700 MHz with fixed capacitors raise the challenge of the component insertion loss. Distribution of the tuning capacitance is investigated and shows 1 dB improvement in the antenna radiation efficiency.

1. Introduction

The need for bandwidth has been dramatically increased with the standardization of the 4th Generation (4G) of mobile communication systems. Handset devices need to cover an ever-increasing frequency spectrum. Today's specifications fill the spectrum from 700 MHz to 2.6 GHz [1]. The trend shows that further widening of the spectrum towards 600 MHz is likely. Therefore, the need for frequency coverage is urgent and essential to future communication systems. However, electrically small antennas respond to fundamental laws that limit their possibility to increase their bandwidth while simultaneously preserve a small size and a good radiation efficiency. The trade-off between antenna radiation efficiency, size and bandwidth is detailed in [2]. The antenna bandwidth issue is mostly challenging at the low frequencies (below 1 GHz) as the radiating structure is the whole handset, which becomes electrically smaller.

In order to cover the required bandwidth, Frequency Reconfigurable Antennas (FRA) are a promising solution. An FRA is a small and efficient antenna that covers only one band at a time. This element is made reconfigurable in order to choose which band to operate in. In that way, FRA can cover an effectively wide bandwdith—while covering instantaneous narrow bandwidths—and preserve its small size. Further, one can see that the complexity of the RF chain increases with the number of bands to cover, and an optimal solution is having an antenna pair (separate and flexible transmitting and receiving chains). In that case, one FRA only needs to cover a channel, which decreases even further its bandwidth requirement, highlighting FRA potential for 4G communication systems.

The reconfigurability mechanism can be implemented with various techniques such as switches, p-i-n or varactor diodes [3], or MicroElectroMechanical Systems (MEMS) capacitors. MEMS components are regarded as the best candidates for FRA application as they exhibit a high Quality factor (Q) and excellent linearity. They add little insertion loss in Radio Frequency (RF). For example, RF MEMS tunable capacitors have been successfully implemented in tunable filters, as described in [4–6]. Their implementation on mobile phone antenna designs has been investigated in [7] and in [8] for the UHF band (510 MHz–800 MHz) and in [9] for the PCS and IMT bands. RF MEMS appeared for the first time on the phone market with the release of Samsung Omnia [10].

The first study on the antenna pair front-end design [11] shows the importance of the Q of the tuning capacitor as it severely affects the FRA radiation efficiency. Further studies on FRA confirm that the limiting criteria to achieve highly efficient systems are the tunable component. In [8], MEMS

variable capacitors are used to tune a low-profile antenna in the Digital Terrestrial Broadcasting (DTB) band. The efficiency decreases from −1 dB to −4 dB between 800 MHz and 500 MHz. This study is relevant as the investigated frequencies can be foreseen as the next ones and most challenging ones to be covered with 4G.

The losses in FRA are mainly coming from the tuner and need to be overcome eventhough better components are not yet available. This paper investigates the loss mechanism of the FRA at the low-band and proposes a distributed tuning mechanism in order to reduce the loss due to the tuner. The paper will be organized in 5 sections. Section 2 presents the problem of high-loss for fine-tuned narrowband antennas. Section 3 details the distributed-tuning design, and Section 4 concludes on the improvements such design brings on the antenna performance. Finally, Section 5 describes the future implementation of the presented findings.

2. Problem Formulation

The FRA must have the ability to be fine-tuned over the bands to cover. This study focuses on the low-band for 4G from 960 MHz to 700 MHz. As detailed in [12], in order to achieve fine-tuning, the capacitance steps of the tuner will determine the position of the tuner on the antenna structure. The total tuning range will then be determined by the maximum capacitance the tuner can provide. Moreover, the position of the tuner will determine the loss it will cause on the total antenna system. It is important to understand that the optimal position of the tuner—that is determined by its capacitance steps—is not the optimal position from an efficiency point of view [13]. The closer to the antenna feed point, the higher the currents delivered to the tuner and the greater the loss. Indeed, the tuner has resistive losses; they are modeled with the Equivalent Series Resistance (ESR) and are proportional to the square of the current delivered to it. As a result, the measured loss becomes greater as the antenna is tuned further away from its original resonance frequency. This loss issue is a specific problem of fine-tuned narrowband antennas and it has been documented in [8, 12, 14–17] with different tuning components. Additionally, the work in [18] uses high-Q discrete components instead of a packaged tuner and shows that the same phenomenon happens. The total loss drops from −2.2 dB to −3.6 dB between 960 MHz and 800 MHz. As documented in the literature, the greatest loss happens at the furthest frequency the antenna is tuned to, compared to its natural resonance frequency. Therefore, the investigation presented in this paper will focus on the lowest frequency of the tuning range, here 700 MHz. This section will present two antenna mock-ups and measure their efficiency. The first mock-up includes a discrete high-Q capacitor and the second mock-up includes a built-in air capacitor. This study will quantify the loss due to the fixed capacitor. The next section will propose a distributed tuning system in order to reduce that loss.

2.1. Antenna Design. The presented antenna design aims at being assembled with an MEMS tunable capacitor to become an FRA. For that reason the design is made to originally resonate at 960 MHz. Simulations were performed with the transient solver of CST MWS, a Finite-Element-Method-(FEM-) based solver [19]. The chosen design is a Planar-Inverted-F Antenna (PIFA) as it is a low-cost and easy to manufacture antenna. The dimensions of the PIFA are shown in Figure 1. The ground plane of the structure has dimensions 120 × 55 mm in order to represent nowadays smartphones. The PIFA is placed 2 mm above the ground plane. The port 1 represents the feeding point of the antenna and the port 2 represents the tuning capacitor. Port 1 and Port 2 are spaced by 14 mm. The short of the PIFA is placed 2 mm below the feeding point. Simulations can determine the position of the tuner in order to achieve fine tuning with capacitance steps of 1/8 pF—as provided by the tuner in [20]. Key information in the design of an FRA is that the capacitance steps of the tuner will determine the position of the tuner on the antenna structure in order to achieve fine-tuning. To continuously tune the resonance frequency of the proposed antenna to 700 MHz, a total capacitance of 5.1 pF is needed, at the position 14 mm away from the source. Simulations of the tunability of the antenna design are shown in Figure 2. In lossless simulations the matching of the antenna varies as more capacitance is added to the structure. In measurements,

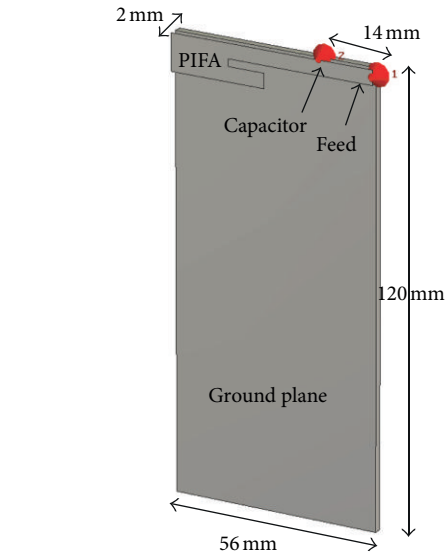

(a) Antenna

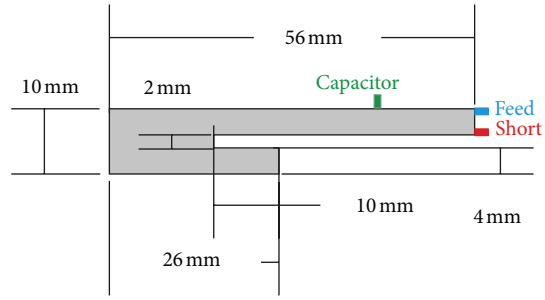

(b) PIFA dimensions

Figure 1: Antenna design.

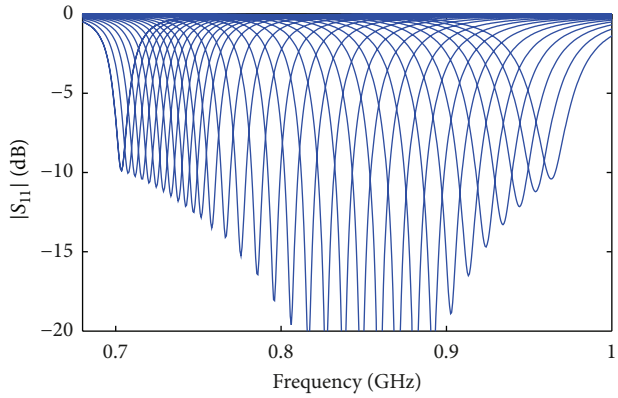

Figure 2: Simulated FRA frequency response.

Table 1: ESR and Q_c of the discrete capacitor at 700 MHz.

C [pF]	ESR [Ω]	Q_c
5.1	0.258	173

the tuning loss helps preserving the matching [12]. This phenomenon will also be shown in the next subsection.

2.2. Discrete-Capacitor-Based FRA. The design previously described is built with a discrete capacitor for resonating at 700 MHz and it is shown in Figure 3. The mock-up is made out of pure copper and minimum tin is used in order to isolate the loss due to the ESR of the capacitor only. The high-Q Murata [21] fixed capacitor is inserted between the PIFA and the GP. The ESR and Q of the capacitor (Q_c) are summarized in Table 1. Q_c is calculated according to (1) where ω is the angular frequency and C is the capacitance:

$$Q_c = \frac{1}{\omega \times C \times \mathrm{ESR}}. \quad (1)$$

Frequency responses of the mock-up are measured with and without fixed capacitor. Figure 4 shows that the matching is preserved throughout tuning. Additionally, the bandwidth (at −6 dB) is reduced from 25 MHz to 10 MHz. This is a result of the Antenna Q (Q_A) that dramatically increases as the resonance frequency is tuned further away from its natural one, as explained in [22]. The measured Q_A is depicted in Figure 5 and shows an increase from $Q_A = 25$ without tuning capacitor to $Q_A = 90$ with tuning component. The mock-up is further measured in anechoic chamber and its peak efficiency at resonance is computed with 3D pattern integration technique. The measured radiation efficiency (η_r) is −3.4 dB. η_r reflects only the thermal loss and the ESR loss. Mismatch and cable losses have been taken out hereafter.

2.3. Air-Capacitor-Based FRA. Narrowband antennas have a loss mechanism that is more complex than only the loss due to the ESR of the tuning capacitor, as shown in [12]. In order to isolate the thermal loss due to the narrowband antenna design itself, the previous mock-up is rebuilt with an integrated air capacitor made out of the same copper piece as the rest of the antennas. The efficiency measurement will show the loss exclusively due to the copper. Figure 6 shows the pure copper mock-up. The two relatively small metal plates forming the air capacitor have the dimensions 20 × 10 mm. The size of the built-in air capacitor is calculated with (2) where ϵ is the permittivity, A is the area, and d is the distance separating the two plates. The capacitor is supported with additional polystyrene in order to have a stable distance d. Expanded polystyrene foam is commonly used in antenna mock-ups because its effect on measured antenna properties is known to be very low. The relative permittivity of the material used in the following is about 1.03 [23, 24]:

$$C = \frac{\epsilon A}{d}. \quad (2)$$

The air capacitor adds radiation surface to the mock-up and raises the question of comparability between the air-capacitor and the fixed capacitor mock-ups. In order to verify whether the air-capacitor alters the radiation characteristics of the antenna, the envelope correlation (ρ) is computed, as defined in [25]. It compares the measured pattern of the mock-up with the fixed capacitor and the measured pattern of the mock-up with the built-in air-capacitor. The anechoic chamber measurement is performed with angular steps of 15 degrees and $\rho = 0.988$. It is concluded that both mock-ups are comparable. The air capacitor acts as the discrete component-storing energy-and not as a radiator. Additionally, it is located at the top of the mock-up, where the fields are minimum according to dipole radiation mode. The measured radiation efficiency of the air-capacitor-based mock-up is $\eta_r = -0.8$ dB.

2.4. Mock-Up Resonating at 700 MHz. In order to confirm the existence of high thermal loss for pure-copper-narrowband antennas, a third mock-up resonating at 700 MHz is built. The modification made to the design shown in Figure 1 is lengthening the bottom arm of the PIFA from 26 mm to 56 mm. The new antenna exhibits similar complex antenna impedance and the radiation efficiency measurement shows $\eta_r = -0.8$ dB.

2.5. Interpretation of the Results. Antenna thermal loss due to the copper conductivity exists and plays a nonnegligible role in narrowband antenna designs. It cannot be easily simulated as shown in [26]. However, it can be isolated and measured. Once this loss is taken out of the FRA radiation efficiency, the loss due to the fixed component only can be evaluated. Comparing the discrete component measurement and the air capacitor measurement leads to the conclusion that the loss due to the ESR of the tuning capacitor is equal to −2.6 dB (−3.4 − (−0.8)). This result matches simulated loss due to the ESR. Indeed, the currents delivered to the tuning capacitor (I_C) can be computed in the simulator, and according to (3) it can be calculated that the dissipated Power due to the ESR (P_L) equals −2.3 dB. The estimated loss matches well the measurement as the difference between them is within the chamber accuracy:

$$P_L = \frac{I_C^2 \times \mathrm{ESR}}{2}. \quad (3)$$

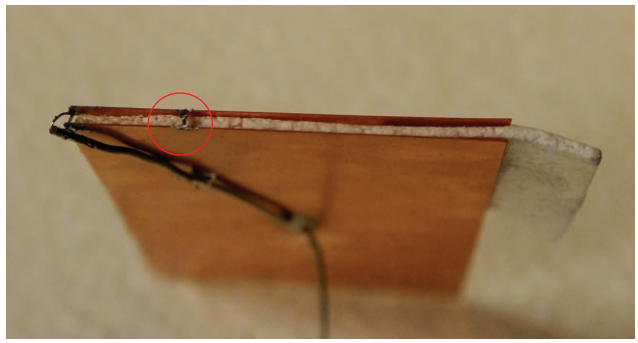

Figure 3: FRA mock-up with discrete capacitor.

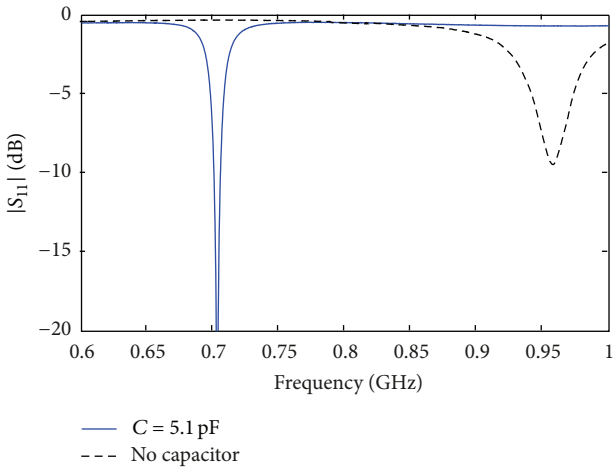

Figure 4: Measured FRA frequency response.

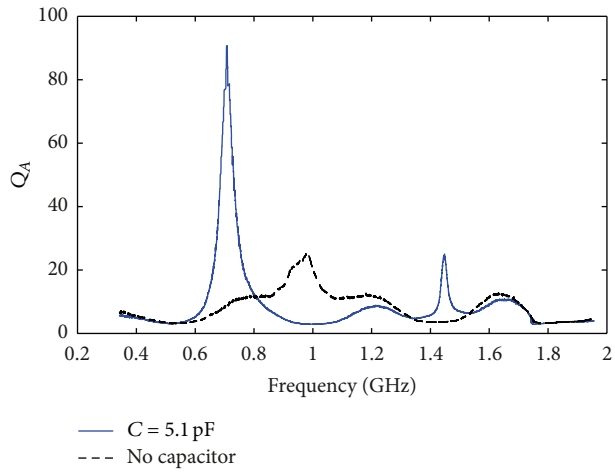

Figure 5: Measured Q_A of FRA with and without discrete capacitor.

The following section of this paper addresses the possibility of reducing P_L with a distributed capacitance design.

3. Distributed Tuning

It is well understood that by distributing the tuning mechanism along the antenna plate the current delivered to each

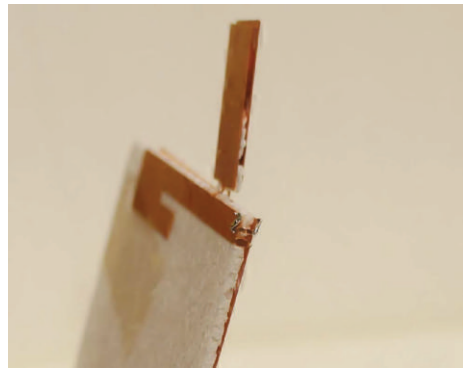

Figure 6: FRA mock-up with air capacitor.

capacitor would be reduced, and so the loss. However, how the distribution should be designed is not an obvious choice. This section presents how to place the tuners and investigates the loss reduction with simulations and measurements.

3.1. Design. Two tuning capacitors are used instead of one. They are both placed between the antenna element plate and the GP plate. Their location is chosen according to the capacitance steps the tuners can provide. According to the previous sections, a capacitor providing steps of 1/8 pF needs to be placed 14 mm away from the source on the investigated PIFA design in order to achieve fine-tuning over the targeted bands. With a distributed design, one of the capacitors also needs to be placed at 14 mm in order to ensure fine-tuning, given that it provides steps of 1/8 pF as well. The other capacitor can be placed further away from the source. The additional capacitor will then tune with larger frequency shifts. In that way, the first tuner C_1 (placed the closest from the source) will use smaller amounts of capacitance compared to a single tuner design. This will result in less loss due to its ESR. The second tuner C_2 (placed the furthest from the source) will also exhibit low loss, as it is placed far from the high-current concentration.

Figure 7 illustrates the distributed-tuning design that is implemented on the investigated PIFA design. The results obtained with the distributed capacitance design shown in Figure 7(a) will be compared to the case where only one tuning capacitor is used at 14 mm from the source

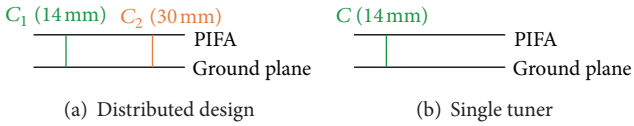

(a) Distributed design (b) Single tuner

Figure 7: Tuning designs.

Table 2: Capacitance and ESR for distributed tuning.

	$C_{1\text{pos}}$ = 14 pF/Ω	$C_{2\text{pos}}$ = 30 pF/Ω
900 MHz	0.250/0.863	0.250/0.863
850 MHz	0.375/1.120	0.625/0.282
800 MHz	1.000/0.325	0.875/0.298
750 MHz	1.500/0.230	1.250/0.282
700 MHz	2.000/0.197	1.750/0.244

Table 3: Capacitance and ESR for single-capacitor tuning.

	C_{pos} = 14 mm pF/Ω
900 MHz	1.000/0.336
850 MHz	2.000/0.212
800 MHz	3.000/0.234
750 MHz	4.000/0.243
700 MHz	5.125/0.257

(C_{pos} = 14 mm) as shown in Figure 7(b). This comparison will lead to a fair evaluation of the improvement a distributed-tuning mechanism brings to an FRA. From a reflection coefficient point of view, performances are unchanged with a distributed system compared to a single-capacitor tuning system.

3.2. Simulations. The investigation on the distributed capacitance is first conducted with simulations. The ESR of the simulated capacitors is taken according to the bank of Murata 0402 capacitors from the GRM 15 collection [21], values for the MEMS [20] not being available. All the simulations are normalized to 1 W input power.

3.2.1. Capacitance. Tables 2 and 3 summarize the capacitance and ESR data that will be used throughout the simulations, in order to tune the investigated PIFA design from 960 MHz to 700 MHz. For more clarity, the simulated results are only displayed every 50 MHz. Tables 2 and 3 also show that by using the distributed design, the amount of capacitance that is needed per capacitor is considerably smaller than that with using only one tuning capacitor. Indeed, if only one capacitor was used for tuning at the position C_{pos} = 14 mm, the amount of required capacitance at this location would be at least twice larger than that with the proposed distributed design.

3.2.2. Normalized Currents. The surface currents in the case of single-capacitor tuning and of distributed tuning are shown in Figure 8 for 700 MHz. In the case of the distributed tuning, the currents are spread on a larger section. Figure 9 depicts the magnitude of the peak current at each capacitor. It compares the distributed system to the single-capacitor tuning system. At 700 MHz in the case of the distributed tuning, the currents delivered to C_1 are reduced by 65% compared to the case of the single-capacitor tuning. The additional capacitor C_2 receives currents that are 50% reduced compared to the single-capacitor case. This significant current reduction will lead to a significant loss reduction.

3.2.3. Dissipated Power in the ESR. The amount each capacitor needs to provide to tune the antenna to a certain frequency is minimized with the use of a distributed-tuning system. Consequently, the energy stored in each capacitor is considerably reduced by using a distributed system. This result is plotted in Figure 10. Hence, the dissipated power in the ESR of each capacitor is also reduced using a distributed system, as depicted in Figure 11. At 700 MHz, the power dissipated by the capacitor placed at 14 mm is divided by a factor 4 for the distributed tuning compared to the single-capacitor tuning mechanism. The simulated η_r can be computed with the ESR values from Tables 2 and 3 and the simulated conductive loss. The conductive loss is a difficult task to model, requiring an extremely fine mesh in the transient simulator [26]. It is often under-estimated. The Figure 12 plots the simulation results of η_r over frequency. For the single-capacitor tuning system, an improvement of 1.5 dB happens due to the ESR loss alone, simulated radiation loss being identical for both mock-ups.

3.3. Interpretation of the Results. Distributed tuning has been compared to single-capacitor tuning with simulations. Given a capacitance step of the tuner, there is only one position (measured in distance to the antenna feed point) that will provide fine tuning. The same position must be taken by one of the capacitors used for distributed tuning. The second capacitor can be placed further away from the feed, at an arbitrarily chosen position. The main advantage that distributing the tuning provides to FRA is that the loss reduction increases as the antenna is tuned further away from its natural resonance (here 960 MHz). The further the antenna is tuned, the more relevant the distribution is. At 700 MHz, the dissipated power by the ESR is already reduced by a factor 4, and the radiation efficiency is enhanced by 1.5 dB using distributed tuning. With a trend towards extending the frequency spectrum to even lower frequencies, distributing the tuning will bring significant efficiency improvements. Using more than two capacitors to even further distribute the tuning could be considered. Nevertheless, one must keep in mind that the ESR increases as the capacitance decreases. Therefore, it is a trade-off between the reduction of the current density by distributing the tuning and the increase of the ESR by using smaller amounts of capacitance. Further investigations on the proposed design have shown that distribution with two capacitors is the optimal design.

3.4. Measurement. The mock-up shown in Figure 3 is modified for the distributed-tuning measurement. Instead of one capacitor of 5.1 pF placed at 14 mm from the feed, two

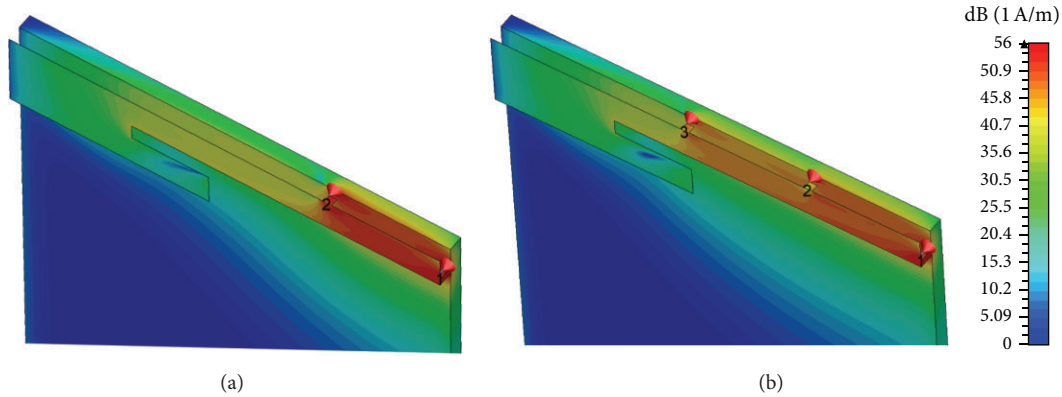

FIGURE 8: Surface currents in a single-capacitor tuning system (a) and a distributed system (b). Port 1 is the feed, port 2 and port 3 represent the capacitors.

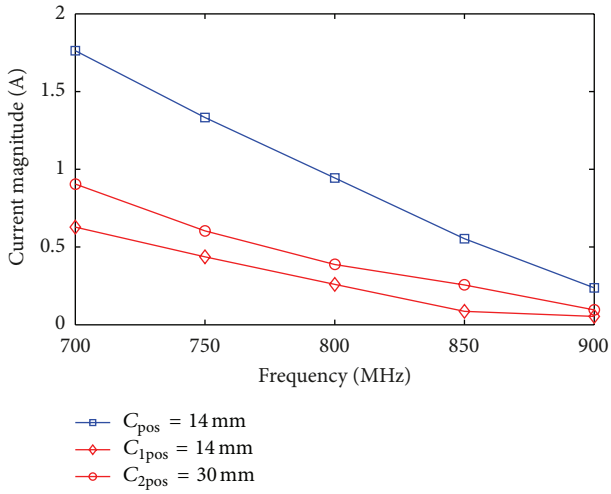

FIGURE 9: Normalized currents in a single-capacitor tuning system and a distributed system.

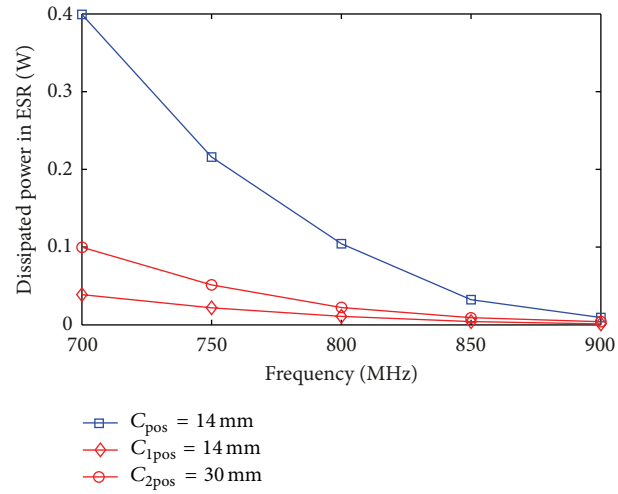

FIGURE 11: Dissipated power per capacitor in a single-capacitor tuning system and a distributed system.

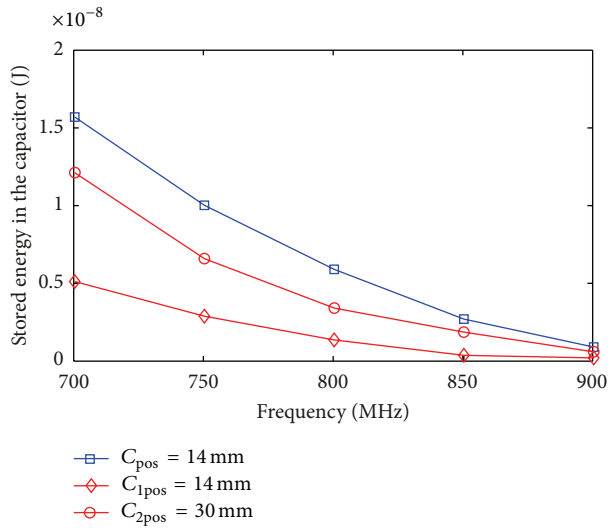

FIGURE 10: Energy stored in each capacitor in a single-capacitor tuning system and a distributed system.

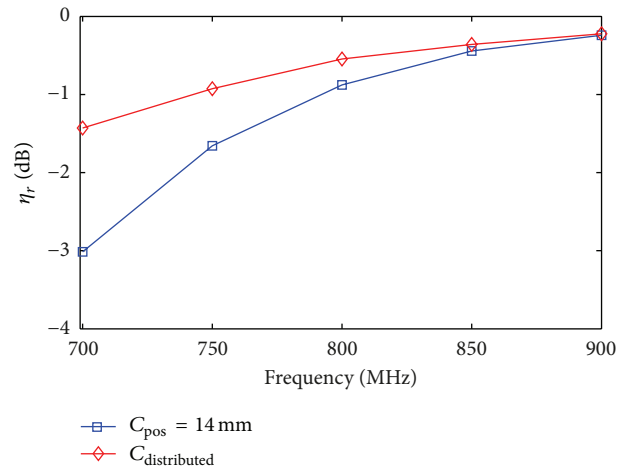

FIGURE 12: Simulated radiation efficiency in a single-capacitor tuning system and a distributed system.

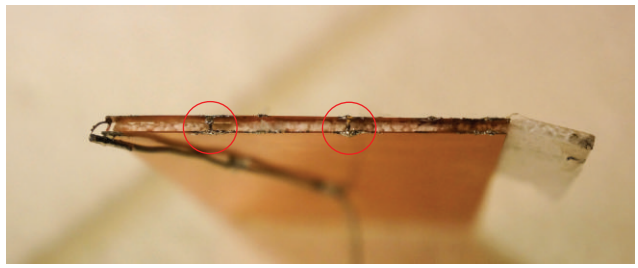

Figure 13: FRA mock-up with distributed tuning system.

capacitors are used as shown in Figure 13. According to the Table 2, the capacitor placed at 14 mm takes the value 2.0 pF and the capacitor placed at 30 mm takes the value 1.7 pF. The frequency response of the mock-up is comparable to the one of the single-capacitor mock-up in terms of resonance frequency and bandwidth. The unloaded Q_A is not affected by having one or two capacitors on the mock-up. However, the measured loaded Q_A is increased by 20%, due to ESR adding in parallel. This increase corresponds to a bandwidth reduction of less than 1 MHz; therefore, it is considered negligible. The mock-up is further measured in anechoic chamber and the radiation efficiency equals $\eta_r = -2.1$ dB. With only one capacitor, the measured radiation efficiency is $\eta_r = -3.4$ dB. This measurement shows an improvement of 1.3 dB on the antenna efficiency when two capacitors are used instead of one. This result is consistent with the simulated improvement.

4. Conclusion

This work has highlighted the issue of tuning loss for narrowband FRA. This type of antennas can provide continuous tuning over a large frequency range. They have a great potential for 4G communications as only one small element can cover all frequencies in the low band (700 MHz to 960 MHz), by being tuned to the desired band (or channel if one considers an antenna pair). However, the tuning component cannot be placed in the best location from an efficiency point of view. That is because the position of the tuner ensures the fine tuning. As the loss it causes on the antenna radiation efficiency is significant—due to high fields in narrowband antennas—it is crucial to understand and reduce its impact. This work is specific to fine-tuned narrowband antennas, as for a 2-stage frequency reconfigurability there is more flexibility in the choice of the tuner position. Tuning has been considered to be performed with an MEMS variable capacitor in simulations. For more practicality, measurements have been performed with high-Q fixed components.

The conclusion of this paper is twofold: firstly, it shows the existence of thermal losses for narrowband antennas; secondly the loss due to the ESR of the tuner is quantified and reduced using a distributed-tuning mechanism. The antenna thermal loss (due to conductivity of the copper plate) is nonnegligible for narrowband antennas. This phenomenon happens because narrowband antennas exhibit higher and more confined fields than typical antennas. Additionally, the higher thermal loss needs to be measured, as its estimation using simulators cannot be achieved in reasonable computational time. This paper compares a built-in air capacitor to a fixed high-Q component in order to quantify the loss due to the ESR of the capacitor and the thermal loss. In this way, the measured loss due to the ESR matches the simulated one. The ESR loss was estimated to be 2.6 dB when the antenna was tuned from 960 MHz to 700 MHz. In order to reduce this loss, a distributed-tuning design is proposed. It uses two capacitors placed at two different locations on the antenna. At 700 MHz, the distributed tuning shows 1.3 dB improvement on the total loss compared to the single-tuning mechanism. The loss due to the tuner increases as the operating frequency is tuned towards lower values. Similarly, the loss reduction improves as the frequency is tuned further away from the natural resonance frequency of the design. The wider the tuning range is, the greater the improvement by distributing the tuning.

5. Future Work

Distributing the capacitance reduces the current in each tuner. The voltage will be increased and one needs to ensure that it remains below the breakdown voltage of the tuner. However, with MEMS technology the breakdown voltage and the maximum capacitance are a trade-off. As distributing the tuning involves lowering the maximum capacitance, simultaneously increasing the maximum handled voltage should not be an issue. Moreover, designing a distributed-tuning mechanism increases the degree of complexity of the antenna, as two tuners are needed instead of one. Therefore, the authors suggest to co-design the antenna and the tuner so that only one tuner with two parallel and independent tracks can be used, instead of two tuners. Cost and complexity reduction can then be achieved and an efficient FRA can be manufactured for 4G. In the future work, the authors will build an FRA with a specifically designed tuner in order to efficiently cover the low band of the 4G spectrum with a single and small antenna.

Acknowledgment

The work is supported by the Smart Antenna Front End (SAFE) Project within the Danish National Advanced Technology Foundation, High Technology Platform.

References

[1] "Feasibility study for further advancements for E-UTRA (LTE-Advanced)—Specification 36. 912—Release 11," 3GPP Technical Report, 2012.

[2] R. F. Harrington, "Effect of antenna size on gain, bandwidth, and efficiency," *Journal of Research of the National Bureau of Standards D*, vol. 64, no. 1, pp. 1–12, 1960.

[3] S.-K. Oh, H.-S. Yoon, and S.-O. Park, "A PIFA-Type varactor-tunable slim antenna with a PIL patch feed for multiband applications," *IEEE Antennas and Wireless Propagation Letters*, vol. 6, pp. 103–105, 2007.

[4] A. Abbaspour-Tamijani, L. Dussopt, and G. M. Rebeiz, "Miniature and tunable filters using MEMS capacitors," *IEEE Transactions on Microwave Theory and Techniques*, vol. 51, no. 7, pp. 1878–1885, 2003.

[5] D. Peroulis, S. Pacheco, K. Sarabandi, and L. P. B. Katehi, "Tunable lumped components with applications to reconfigurable MEMS filters," in *Proceedings of the International Microwave Symposium Digest IEEE-MTT-S*, pp. 341–344, May 2001.

[6] Y. Liu, A. Borgioli, A. S. Nagra, and R. A. York, "Distributed MEMS transmission lines for tunable filter applications," *International Journal of RF and Microwave Computer-Aided Engineering*, vol. 11, no. 5, pp. 254–260, 2001.

[7] M. Nishigaki, T. Nagano, T. Miyazaki et al., "Piezoelectric MEMS variable capacitor for a UHF band tunable built- In antenna," in *Proceedings of the IEEE MTT-S International Microwave Symposium (IMS '07)*, pp. 2079–2082, June 2007.

[8] Y. Tsutsumi, M. Nishio, S. Obayashi et al., "Low profile double resonance frequency tunable antenna using RF MEMS variable capacitor for digital terrestrial broadcasting reception," in *Proceedings of the IEEE Asian Solid-State Circuits Conference (A-SSCC '09)*, pp. 125–128, November 2009.

[9] J. R. De Luis, A. Morris, Q. Gu, and F. de Flaviis, "Tunable duplexing antenna system for wireless transceivers," *IEEE Transactions on Antennas and Propagation*, vol. 60, pp. 5484–5487, 2012.

[10] "Teardown: Samsung Focus Flash," http://evertiq.com/news/21198?utm%20source=feedburner&utm%20medium=feed%20&utm%20campaign=Feed%253A+EvertiqCom%252FAll+28evertiq.com+%253A%253A%20+Latest+news%2529&utm%20content=Google+Reader.

[11] J. T. Aberle, S.-H. Oh, D. T. Auckland, and S. D. Rogers, "Reconfigurable Antennas for Portable Wireless Devices," *IEEE Antennas and Propagation Magazine*, vol. 45, no. 6, pp. 148–154, 2003.

[12] S. Caporal, D. Barrio, M. Pelosi, G. F. Pedersen, and A. Morris, "Challenges for frequency-reconfigurable antennas in small terminals," in *Proceedings of the IEEE Vehicular Technology Conference (VTC Fall '12)*, pp. 1–5, 2012.

[13] S. C. Del Barrio, M. Pelosi, O. Franek, and G. F. Pedersen, "On the currents magnitude of a tunable Planar-Inverted-F Antenna for lowband frequencies," in *Proceedings of the 6th European Conference on Antennas and Propagation (EUCAP '12)*, pp. 3173–3176, March 2012.

[14] M. G. S. Hossain and T. Yamagajo, "Reconfigurable printed antenna for a wideband tuning," in *Proceedings of the 4th European Conference on Antennas and Propagation (EuCAP '10)*, vol. 1, pp. 1–4, April 2010.

[15] A. Suyama and H. Arai, "Meander line antenna built in folder-type mobile," in *Proceedings of the International Symposium on Antennas and Propagation (ISAP '07)*, pp. 294–297, 2007.

[16] V.-A. Nguyen, R.-A. Bhatti, and S.-O. Park, "A simple PIFA-based tunable internal antenna for personal communication handsets," *IEEE Antennas and Wireless Propagation Letters*, vol. 7, pp. 130–133, 2008.

[17] N. Behdad and K. Sarabandi, "A varactor-tuned dual-band slot antenna," *IEEE Transactions on Antennas and Propagation*, vol. 54, no. 2, pp. 401–408, 2006.

[18] S. C. D. Barrio, M. Pelosi, and G. F. Pedersen, "On the efficiency of frequency reconfigurable high-Q-antennas for 4G standards," *Electronics Letters*, vol. 48, no. 16, pp. 982–983, 2012.

[19] Computer Simulation Technology (CST), "CST Microwave Studio," 2012, http://www.cst.com.

[20] WiSpry, "Tunable Digital Capacitor Arrays (TDCA)".

[21] Murata, "Chip Monolithic Ceramic Capacitors," 2012.

[22] O. Kivekäs, J. Ollikainen, and P. Vainikainen, "Frequency-tunable internal antenna for mobile phones," in *Proceedings of the 12th International Symposium on Antennas (JINA)*, vol. 2, pp. 53–56, 2002.

[23] M. A. Plonus, "Theoretical investigations of scattering from plastic foams," *IEEE Transactions on Antennas and Propagation*, vol. 13, no. 1, pp. 88–94, 1965.

[24] E. F. Knott, "Dielectric constant of plastic foams," *IEEE Transactions on Antennas and Propagation*, vol. 41, no. 8, pp. 1167–1171, 1993.

[25] J. Pierce and S. Stein, "Multiple diversity with nonindependent fading," *Proceedings of the IRE*, vol. 48, pp. 89–104, 1960.

[26] S. Caporal Del Barrio and G. F. Pedersen, "High-Q antennas: simulator limitations," in *Proceedings of the European Conference on Antennas and Propagation (EuCAP '13)*, vol. 1, 2013.